

Comparing design outcomes of reinforced concrete elements designed using topology optimization

Jackson JEWETT*, Josephine V. CARSTENSEN

*Massachusetts Institute of Technology
77 Massachusetts Avenue, Cambridge MA, USA
jljewett@mit.edu

Abstract

Topology optimization (TO) is a design optimization method known to generate high-performing structures with a limited volume of material. TO has great potential in the construction industry because it can help reduce the use of building materials, which produce approximately 10% of greenhouse gasses worldwide. Within existing research on TO for construction, tailoring algorithms specifically to reinforced concrete (RC) design has received considerable attention. This research presents a new framework for topology optimization of RC. Continuum elements in compression and truss elements in tension are used together to represent concrete and steel, respectively. The locations of the nodes of the truss elements are controlled by design variables, and moved during the optimization process. Also, SIMP penalization schemes are not used on the continuum elements, so that their respective design variables can take intermediate values between 0 and 1. These values are interpreted as varying thicknesses in the final design, following the Variable Thickness Sheet method. The performance of numerical design examples is compared herein, so that optimized designs can be fabricated and tested to demonstrate their efficacy in future work.

Keywords: Topology optimization, digital concrete, reinforced concrete design, structural optimization, low weight design

1. Introduction

Topology optimization (TO) of reinforced concrete (RC) is an important field of research because it has potential to reduce the high Carbon emissions of the construction industry, which are estimated to make up 10% of all CO₂ emitted globally [1]. TO is a design optimization method known to generate high-performing structures with a limited volume of material [2]. In general, a structural TO is performed on a design space of 2D finite elements, referred to as continuum elements, with isotropic behavior. However, RC is a composite system consisting of both concrete and steel, which have distinct behavioral characteristics. Namely, concrete is strong in compression, but is not effective when acting in tension. For this reason, steel is added to the tension zones of RC structures to resist any relevant tensile forces. Therefore, a TO framework for RC design must capture the relationship between these two materials during the optimization process, and place the concrete and steel appropriately.

There has already been substantial research in TO for design of RC structures [3]. A common approach is to use a TO framework to define strut-and-tie solutions for a RC component, either with continuum or truss elements [4], [5], [6], [7]. Another strategy is to allow the optimization to place two different continuum materials with different stiffnesses in tension and compression [8], [9]. Different Drucker-Prager stress constraints have also been placed two continuum materials to simulate the two materials of RC [10], [11]. Another popular method is to use a combined system of truss and continuum elements,

with trusses representing steel and continuum representing concrete. Following this approach, trusses have been placed in zones where the concrete experiences damage [12], [13]. Alternatively, the stiffnesses of the trusses can be reduced when they are compressive, while the continuum stiffness is reduced when it is in tension [14].

In addition, an exciting new theme of research has been to fabricate and test RC structures designed with TO to experimentally validate the efficacy of the methodology [15], [16], [17], [18], [19].

This research draws heavily from the work of Gaynor et al. [14], and builds on previous publications by the authors [19]. Examples from that research with combined truss and continuum structural systems are shown in Figure 1. The optimization framework presented here is novel because the nodes of the trusses are allowed to move, following the methods from Zegard and Paulino [20]. It also explores the potential of the Variable Thickness Sheet (VTS) method, as highlighted by Sigmund et al. [21].

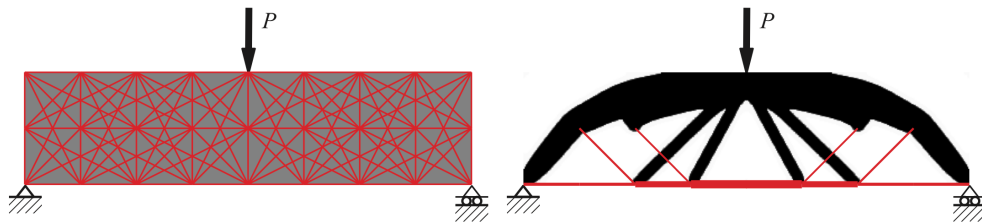


Figure 1: On left, an initial ground structure for a simply supported beam optimization, with truss elements shown in red and the continuum material shown in gray. On right, the optimized result, with continuum material acting in compression and truss elements in tension. This figure is adapted from [19].

2. Methods

This research uses topology optimization (TO) to design low-weight reinforced concrete (RC) elements. RC consists of two materials: concrete acting primarily in compression, and reinforcing steel in tension. The optimization must, therefore, correctly place these two different materials to take the forces within the structural system as efficiently as possible. In this research, the concrete will be designed using continuum elements, and the reinforcement using a truss element discretization. The problem formulation for the optimization is as follows:

$$\begin{aligned}
 \min_{\mathbf{x}_c, \mathbf{x}_t} \quad & c(\mathbf{x}_c, \mathbf{x}_t) = \mathbf{U}^T \mathbf{K} \mathbf{U} \\
 \text{s. t.} \quad & \mathbf{K} \mathbf{U} = \mathbf{F} \\
 & V_c(\mathbf{x}_c) \leq f_c \\
 & V_t(\mathbf{x}_t) \leq f_t \\
 & \mathbf{0} \leq \mathbf{x}_c, \mathbf{x}_t \leq \mathbf{1}
 \end{aligned} \tag{1}$$

Where c is the objective function, which is the compliance in this case. \mathbf{K} is the global stiffness matrix, \mathbf{U} is the displacement vector, and \mathbf{F} is the force vector. V_c is the total volume of continuum material in the system, and f_c is a user-defined constraint on the maximum allowable continuum volume. V_t is the total volume of truss material, and f_t is a user-defined constraint on the maximum allowable truss volume. \mathbf{x}_c is the set of all design variables that control continuum material, and \mathbf{x}_t is the set of all design variables that control truss material.

These design goals are achieved using three strategies. First, a truss-continuum hybrid structural system is used, with force-dependent orthotropy enforced on all members. Additionally, the nodes of the truss elements can be moved by design variables (DVs) with methods that are differentiable. Last, the DVs controlling the placement of continuum elements are not penalized for intermediate densities, so the

Variable Thickness Sheet (VTS) geometries can be obtained. The implementation of these strategies are described below.

2.1. Force-dependent stiffnesses

Enforcement of force-dependent stiffnesses is crucial for RC design. For this research, methods must be used to ensure that continuum elements are favored for compressive forces, while truss members are favored for tension forces. These conditions are enforced by adding an additional step to the optimization loop. In this new step, the stiffnesses of the truss and continuum elements are defined through an iterative process depending on their internal forces, as shown in Figure 2a. Essentially, this adds an inner loop to the beginning of each step of the optimization loop.

The method for assigning the truss stiffness is straightforward. For each truss element, the displacement of each of its two nodes is calculated as an interpolation of their 4 nearest continuum nodes. If the deflection between these interpolated values is positive, the element has tensile stress, while if the deflection is negative, the stress is compressive. Tensile elements are assigned a high elastic modulus value, while compressive elements are assigned a very low value approaching zero, shown in Figure 2b and 2c.

The continuum elements are two dimensional, and the higher dimensionality leads to more complexity in how stiffnesses are assigned. When the FEA is performed, the stresses in each element can be calculated. For a 2D structure, each element has a stress in the X and Y direction, σ_x and σ_y , and a shear stress, σ_{xy} , as shown in Figure 2d. Principal stresses can be calculated from these global stress values, which are equivalent normal stresses with associated shear stresses of zero. Principal stresses also have a corresponding principal angle, θ . These are illustrated in Figure 2e. In this work, the principal stresses of each element are calculated, and the local stiffness matrix of the element K_e is modified based on their directionality. If the principal stress is negative, a high stiffness is assigned in the corresponding direction, and if it is positive, and low stiffness is assigned.

The stiffness values for truss and continuum elements in tension and compression correspond to those shown in Figure 2a. It should be noted that the values used do not reflect the true stiffnesses of concrete and steel, but rather allow the optimization to converge on useful results.

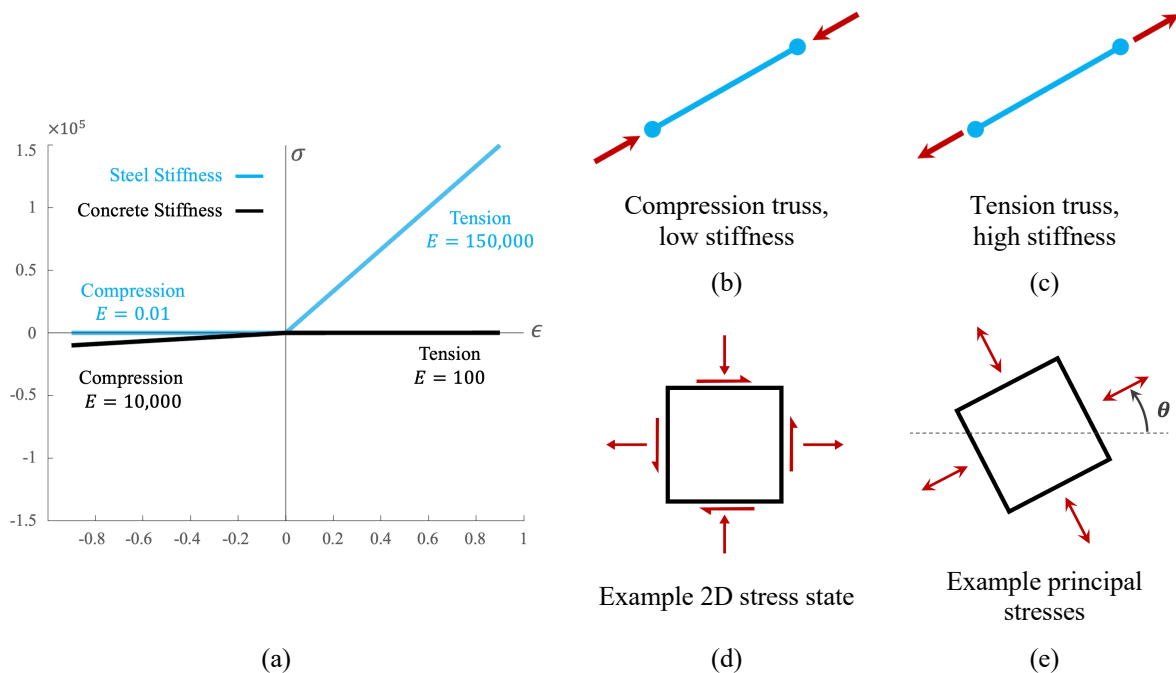


Figure 2: in (a), the stiffnesses of continuum and truss members under tension and compression are shown graphically. (b) and (c) show how the stress states on truss elements are used to assign appropriate stiffnesses. A

possible stress state of a continuum element in global coordinates is shown in (d), with a depiction of principal stresses and principal angle for stiffness assignment shown in (e).

Within this inner loop, a finite element analysis (FEA) is performed first assuming all elements have high stiffness. Based on the results, the stiffnesses of all elements are updated based on the directionality of their internal forces. Updating the stiffnesses will change the results of the FEA, so the process must be repeated until those changes are very small. In the case of this research, the loop is stopped when the change of the compliance of the system between iterations is less than 0.1%. This process follows the framework outlined in Gaynor and Guest [14] and Du et al. [22], which has been used in continuum topology optimization [23]. Readers are referred to these works for more detail. After this initial loop converges, the optimization continues as usual using the found stiffnesses.

2.2. Variable thickness sheet

In density-based TO, which is used in this research, continuous design variables (DVs) that can take values between 0 and 1 are used to control the placement of material. Usually users seek a “0-1” solution, in which intermediate design variable values are penalized, so the optimization specifies areas where material should be placed with variable values of 1, and areas where it should be taken away with values of 0. However, research has shown that these 0-1 outputs can often produce low-performing structures relative to other design methods [21]. Sigmund et al. proposes that, rather forcing 0-1 outputs in TO, it can be better to use the Variable Thickness Sheet (VTS) method, in which the thicknesses of the structure are controlled directly by continuous variables without penalization of intermediate values.

This research uses VTS by interpreting design variable values directly as thicknesses [2]. A DV value of 1 would be interpreted as a maximum thickness, a value of 0 would mean no material is placed, and any values in-between are interpreted as a linear interpolation. Examples of this approach are shown in Figure 3.

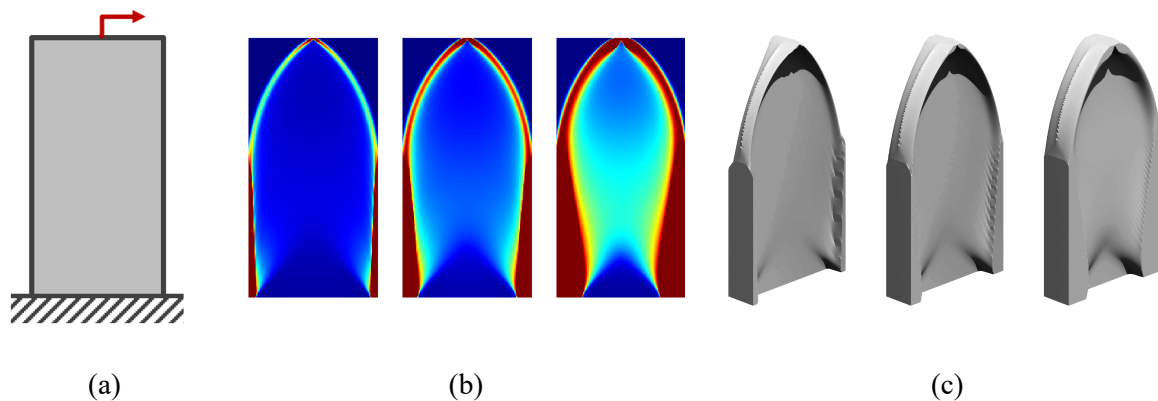


Figure 3: For a vertical cantilever loadcase (a), results with volume restrictions of 0.15, 0.3, and 0.5 allowing for continuous variable values are shown in (b). The variable sheet interpretations of these results with a cutoff density threshold of 0.001 are shown in (c). This figure is based on that of Sigmund et al [21].

2.3. Moving trusses

In addition to the use of VTS method, this research also expands on previous work by allowing the nodes of truss elements to move during the optimization process. This process is visualized conceptually in Figure 4.

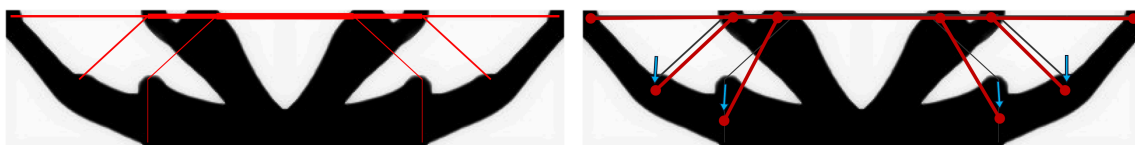


Figure 4: On left, a truss-continuum hybrid optimization output with static truss nodes. On right, an example of how moving the truss nodes might improve the performance of the design, with blue arrows showing possible movement paths.

The most challenging aspect of this added flexibility is ensuring that the stiffness of truss elements is transferred properly to the nearby continuum elements. Normally in FEA, element nodes must land identically on top of one-another. However, if the location of the truss nodes is controlled by continuous DVs, it would be difficult to ensure they land directly on top of the continuum nodes in the system. This is illustrated in Figure 5a. To address this, a stiffness spreading method (SSM) is used, similar to that of Wei et al. [24] and Zegard and Paulino [20]. In SSM, truss elements distribute their stiffnesses to nearby continuum elements within a radius of influence, r . The principal of SSM is illustrated conceptually in Fig. 5d. The stiffness of the truss element is distributed as a function of distance to the nearby continuum nodes using a smooth differentiable function, shown in Fig 5c. Using this method, truss nodes can move continuously throughout the design space while always distributing their stiffnesses to a selection of continuum nodes, like the system illustrated in Fig. 5b.

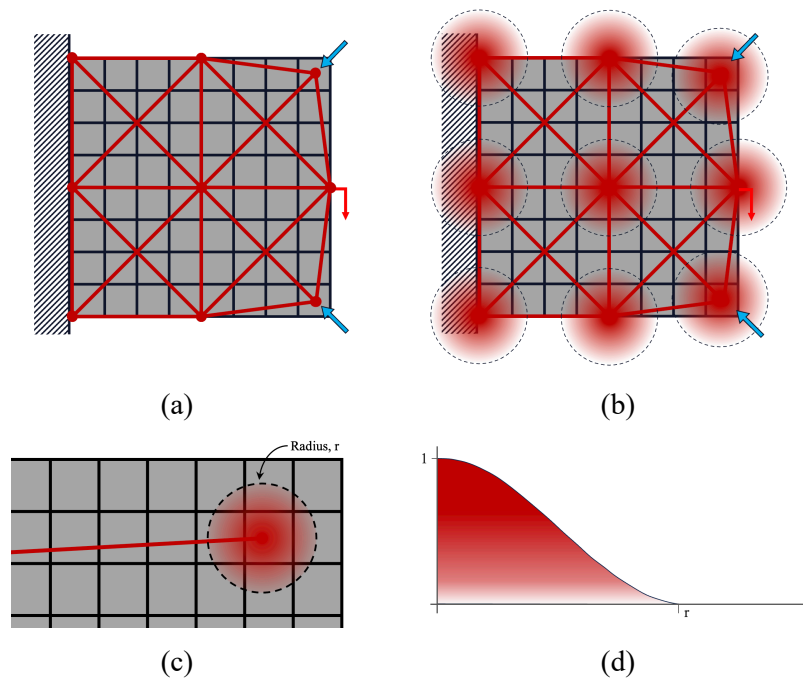


Figure 5: A condition in which truss nodes do not land on top of continuum nodes after being moved by continuous DVs is shown in (a). The use of SSM to distribute truss stiffness to nearby continuum nodes within defined radius r is shown in (c), with an example of the distribution function shown in (d). In (b), the same system as (a) is shown with SSM implemented to allow for the movement of truss nodes with proper stiffness distribution to continuum elements.

3. Results

With these optimization strategies implemented and assembled, it is crucial to evaluate how performance of generated geometries compare to one another. To assess this, 4 geometries are compared that are generated using the same boundary conditions and parameters, with different combinations of design flexibility. The optimizations use either static or moving truss nodes, and 0-1 or VTS continuum elements. The used cantilever load case is visualized in Figure 6. All optimizations use a continuum design space of 110×80 elements, with 2 truss bays in the vertical direction and 3 in the horizontal. The filter radius is set to 3 in all cases, and the SSM distribution radius is set to 4. The truss nodes are able to move 6 elements in any direction, in the cases that allow for movement. The optimizations start with 30 iterations in which the continuum elements are not modified, so that the trusses can be optimized before the material starts to be removed. This is followed by 40 iterations in which truss sizes and

continuum elements can be modified. The truss nodes cannot move during the 2nd phase of the optimization. The 0-1 designs use a penalization variable value of 3. Heaviside projection is not used on any designs. Continuum volume is constrained to 0.4 of the design space, while the truss volume is constrained to 0.15. The results are shown in Figure 7.

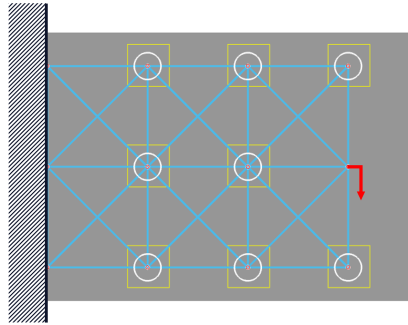


Figure 6: The load case for all designed examples is shown. The blue lines are the truss elements available to the optimization, while the gray is where continuum elements can be controlled. A load is applied in the middle of the right-most truss elements, while all nodes are fixed along the left-hand side. Truss nodes that can be controlled have a yellow square showing the extent to which they can be moved. The red circles show the truss nodes, while the white circles show the radius of the SSM distribution.

	<i>Static Nodes</i>	<i>Moving Nodes</i>
<i>0-1</i>	<p>$C = 16.3861$</p>	<p>$C = 15.8203$</p>
<i>VTS</i>	<p>$C = 16.1947$</p>	<p>$C = 15.6129$</p>

Figure 7: A comparison of compliance values are shown for 4 different optimization conditions. The results in the top row enforce 0-1 outputs, while below the VTS method is used. On left, truss nodes are static, while truss nodes can be moved in the examples on the right.

It can be seen that the design flexibility of VTS and moving truss nodes afford performance gains over the control example with static truss nodes and a 0-1 output enforced. All outputs have lower compliance

values, C , compared to the control case. The compliance of the system is reduced by about 5% using the same volume of material when both strategies are used, which can lead to meaningful gains in built structures.

As described in section 2.2, the gray regions of the VTS designs would be linearly interpreted as thicknesses based on their DV values. The VTS designs could be fabricated with a 2-part symmetric mold that could be filled with concrete and released after an initial cure. Because the design variables only control thickness throughout the design space, it is guaranteed that there will never be internal voids, which eases fabrication. This process is shown conceptually in Figure 8 with a beam example. It should be noted that this fabrication method will not be possible in all building contexts, and may not always lead to reduced construction costs, even though less material is being used.

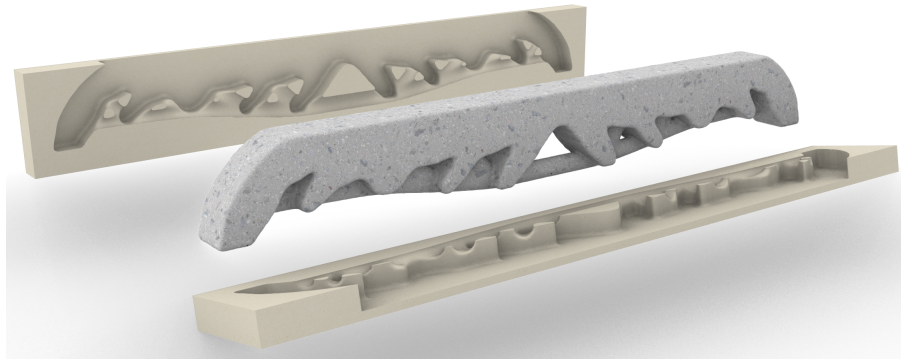


Figure 8: Illustration of a proposed fabrication process for a VTS designed structure. Both pieces of a two-part mold could be placed together to be filled with concrete, which would be released after an initial curing period.

It should be noted that some VTS results would encounter fabrication difficulties following this method. For example, areas of the design space are assigned very low DV values may be so thin that they are difficult to manufacture, and would not carry load in a real-world physical structure. This phenomenon has been observed in other research, such as Giele et al. [25]. Solutions for this problem, such as enforcing a minimum thickness on the VTS design, can be implemented in future work. This would ensure that physical tests can be performed on built specimen.

4. Conclusion

This research uses a hybrid truss-continuum optimization space with force-dependent orthotropy to generate low-weight designs for RC members. The nodes of truss elements are controlled by continuous DVs to move smoothly throughout the design space, and the VTS method is used to vary the thickness at each continuum element. It can be seen that allowing for these added degrees of design flexibility leads to significant improvement in the value of the objective function. This research can inform future work on RC optimization, particularly on best practices for fabrication and testing of experimental structures.

References

- [1] United Nations Environment Programme., “2020 Global Status Report for Buildings and Construction: Towards a Zero-emission, Efficient and Resilient Buildings and Construction Sector.” Nairobi, Kenya, 2020.
- [2] M. P. Bendsøe and O. Sigmund, *Topology Optimization*. Berlin, Heidelberg: Springer Berlin Heidelberg, 2004. doi: 10.1007/978-3-662-05086-6.
- [3] N. Stoiber and B. Kromoser, “Topology optimization in concrete construction: a systematic review on numerical and experimental investigations,” *Struct Multidisc Optim*, vol. 64, no. 4, pp. 1725–1749, Oct. 2021, doi: 10.1007/s00158-021-03019-6.
- [4] Y. Xia, M. Langelaar, and M. A. N. Hendriks, “Optimization-based strut-and-tie model generation for reinforced concrete structures under multiple load conditions,” *Engineering Structures*, vol. 266, p. 114501, Sep. 2022, doi: 10.1016/j.engstruct.2022.114501.

- [5] Y. Xia, M. Langelaar, and M. A. N. Hendriks, “Optimization-based three-dimensional strut-and-tie model generation for reinforced concrete,” *Computer aided Civil Eng*, vol. 36, no. 5, pp. 526–543, May 2021, doi: 10.1111/mice.12614.
- [6] Y. Xia, M. Langelaar, and M. A. N. Hendriks, “A critical evaluation of topology optimization results for strut-and-tie modeling of reinforced concrete,” *Computer aided Civil Eng*, vol. 35, no. 8, pp. 850–869, Aug. 2020, doi: 10.1111/mice.12537.
- [7] M. Bruggi, “Generating strut-and-tie patterns for reinforced concrete structures using topology optimization,” *Computers & Structures*, vol. 87, no. 23–24, pp. 1483–1495, Dec. 2009, doi: 10.1016/j.compstruc.2009.06.003.
- [8] S. Liu and H. Qiao, “Topology optimization of continuum structures with different tensile and compressive properties in bridge layout design,” *Struct Multidisc Optim*, vol. 43, no. 3, pp. 369–380, Mar. 2011, doi: 10.1007/s00158-010-0567-x.
- [9] G. Gaganelis, D. R. Jantos, P. Mark, and P. Junker, “Tension/compression anisotropy enhanced topology design,” *Struct Multidisc Optim*, vol. 59, no. 6, pp. 2227–2255, Jun. 2019, doi: 10.1007/s00158-018-02189-0.
- [10] M. Bogomolny and O. Amir, “Conceptual design of reinforced concrete structures using topology optimization with elastoplastic material modeling,” *Numerical Meth Engineering*, vol. 90, no. 13, pp. 1578–1597, Jun. 2012, doi: 10.1002/nme.4253.
- [11] Y. Luo and Z. Kang, “Layout design of reinforced concrete structures using two-material topology optimization with Drucker–Prager yield constraints,” *Struct Multidisc Optim*, vol. 47, no. 1, pp. 95–110, Jan. 2013, doi: 10.1007/s00158-012-0809-1.
- [12] O. Amir, “A topology optimization procedure for reinforced concrete structures,” *Computers & Structures*, vol. 114–115, pp. 46–58, Jan. 2013, doi: 10.1016/j.compstruc.2012.10.011.
- [13] O. Amir and O. Sigmund, “Reinforcement layout design for concrete structures based on continuum damage and truss topology optimization,” *Struct Multidisc Optim*, vol. 47, no. 2, pp. 157–174, Feb. 2013, doi: 10.1007/s00158-012-0817-1.
- [14] Gaynor Andrew T., Guest James K., and Moen Christopher D., “Reinforced Concrete Force Visualization and Design Using Bilinear Truss-Continuum Topology Optimization,” *Journal of Structural Engineering*, vol. 139, no. 4, pp. 607–618, Apr. 2013, doi: 10.1061/(ASCE)ST.1943-541X.0000692.
- [15] M. Smarslik and P. Mark, “Hybrid reinforcement design of longitudinal joints for segmental concrete linings,” *Structural Concrete*, vol. 20, no. 6, pp. 1926–1940, Dec. 2019, doi: 10.1002/suco.201900081.
- [16] N. Pressmair *et al.*, “Bridging the gap between mathematical optimization and structural engineering: Design, experiments and numerical simulation of optimized concrete girders,” *Structural Concrete*, vol. 24, no. 4, pp. 5314–5330, Aug. 2023, doi: 10.1002/suco.202201096.
- [17] O. Amir and E. Shakour, “Simultaneous shape and topology optimization of prestressed concrete beams,” *Struct Multidisc Optim*, vol. 57, no. 5, pp. 1831–1843, May 2018, doi: 10.1007/s00158-017-1855-5.
- [18] G. Gaganelis and P. Mark, “Downsizing weight while upsizing efficiency: An experimental approach to develop optimized ultra-light UHPC hybrid beams,” *Structural Concrete*, vol. 20, no. 6, pp. 1883–1895, Dec. 2019, doi: 10.1002/suco.201900215.
- [19] J. L. Jewett and J. V. Carstensen, “Experimental investigation of strut-and-tie layouts in deep RC beams designed with hybrid bi-linear topology optimization,” *Engineering Structures*, vol. 197, p. 109322, Oct. 2019, doi: 10.1016/j.engstruct.2019.109322.
- [20] T. Zegard and G. H. Paulino, “Truss layout optimization within a continuum,” *Struct Multidisc Optim*, vol. 48, no. 1, pp. 1–16, Jul. 2013, doi: 10.1007/s00158-013-0895-8.
- [21] O. Sigmund, N. Aage, and E. Andreassen, “On the (non-)optimality of Michell structures,” *Struct Multidisc Optim*, vol. 54, no. 2, pp. 361–373, Aug. 2016, doi: 10.1007/s00158-016-1420-7.
- [22] Z. Du, Y. Zhang, W. Zhang, and X. Guo, “A new computational framework for materials with different mechanical responses in tension and compression and its applications,” *International Journal of Solids and Structures*, vol. 100–101, pp. 54–73, Dec. 2016, doi: 10.1016/j.ijsolstr.2016.07.009.

- [23] Z. Du, W. Zhang, Y. Zhang, R. Xue, and X. Guo, “Structural topology optimization involving bi-modulus materials with asymmetric properties in tension and compression,” *Comput Mech*, vol. 63, no. 2, pp. 335–363, Feb. 2019, doi: 10.1007/s00466-018-1597-2.
- [24] P. Wei, H. Ma, and M. Y. Wang, “The stiffness spreading method for layout optimization of truss structures,” *Struct Multidisc Optim*, vol. 49, no. 4, pp. 667–682, Apr. 2014, doi: 10.1007/s00158-013-1005-7.
- [25] R. Giele, J. Groen, N. Aage, C. S. Andreasen, and O. Sigmund, “On approaches for avoiding low-stiffness regions in variable thickness sheet and homogenization-based topology optimization,” *Struct Multidisc Optim*, vol. 64, no. 1, pp. 39–52, Jul. 2021, doi: 10.1007/s00158-021-02933-z.